on chromosome 17 for 66 of the LOH mutants derived from TK6-20C and 105 of the LOH mutants derived from TK6-E6. Multiplex PCR with a mixture of the 10 primers was performed using genomic DNA from these LOH mutants as template. A representative profile of the PCR products is shown in Fig. 1. Ten pairs of polymorphic marker signals from the multiplex PCR products could be identified in the profile; this enabled us to determine the extent of the various LOH tracts on chromosome 17. The results of the 10 mix multiplex PCR runs for the TK6-20C- and TK6-E6-derived mutants are summarized in Fig. 2. None of LOH mutants (67/110 TK6-20C mutants or 109/117 TK6-E6 mutants) had LOH tracts extending through the D17S932 marker site.

Chromosomal alterations detected among the observed LOH events in TK^- mutants of TK6-20C and TK6-E6 cells (Table 2 and Fig. 2) can therefore be categorized into four classes: point mutations, interstitial deletions, crossing over events, and terminal deletions/translocations. Calculated frequencies of chromosomal alterations seen in this study are presented in Table 3, along with the results of the frequencies observed in our previous study. Frequencies of point mutations, interstitial deletions and crossing over events in TK^- mutants of both cell lines did differ in a small extent (less than twofold) from one study to the next. In contrast, the frequencies of terminal deletions/translocations proved to be much higher (about 60-fold) in TK6-E6 cells than in TK6-20C cells ($P = 0.0001$). In addition the non-disjunction type of chromosome aberration was not observed in this TK6 assay system irrespective of p53 status.

3.3. Mapping of LOH endpoints on chromosome 17q

To map the LOH tracts in more detail along the 45 Mb of chromosome 17q (D17S932 to the telomere), we selected an additional 17 microsatellite markers from the 26 effective markers listed in Table 1 for mapping various LOH endpoints on the defined portion of chromosome 17q; this provides an average map interval of 1.6 Mb (Table 4). The sequence positions of the remaining nine microsatellite markers (Table 1) were so close at the present level of mapping to either one of the flanking markers that we decided not to include the results obtained with any of them. We went on to use the expanded mapping system to analyze 66 of the LOH mutants derived from TK6-20C cells and 104 of the LOH mutants derived from TK6-E6 cells in our present study together with 34 of the LOH mutants derived from TK6-20C cells and 45 of the LOH mutants derived from TK6-E6 cells in our previous study [19]. The results so obtained involved the analysis of 100 TK6-20C and 149 TK6-E6 LOH mutants, and are summarized in Table 4. The LOH endpoints of the TK^- mutants which result from deletions of the *tk* locus as well as those that result from terminal deletions spanning from exon 4 of *tk* to the telomere are depicted together at positions D17S937 to D17S802. The LOH endpoints of a few interstitial deletions which have two endpoints were estimated by the position of the distal ends of the LOH tracts in Table 4. For comparison between the two cell lines, a correction was made for the calculated numbers of LOH endpoints/Mb in TK6-20C by multiplying them in the ratio of analyzed mutant cell numbers (149/100). The estimated relative incidences of LOH endpoints/Mb for both cell lines are shown on the map position of chromosome 17q in Fig. 3, along with the LOH status of each mutant analyzed. There were four prominent peaks of LOH endpoints in TK6-20C cells. Peak I was the most distal from the *tk* locus; the only LOH mutants carrying endpoints at this position were isolated from TK6-20C cells (Table 4). LOH events mapping at peak IV, including *tk* locus deletion mutants, were predominantly of the hemizygous LOH type. The LOH events in TK6-E6 cells were mostly hemizygous, and were rather broadly distributed along the 15–20 Mb length (D17S1807 to D17S1607) of chromosome 17q; they also tended to map around peaks II and III as noted for TK6-20C LOH mutants.

4. Discussion

Although LOH has been studied extensively as a frequently observed symptom of genome instability in cancer cells, the molecular mechanisms underlying its origins have remained obscure. We have described a preliminary characterization of chromosome aberrations and LOH events in spontaneous TK^- mutants from p53-wild type TK6-20C and p53-abrogated cells TK6-E6 [19]. In the present study, we have analyzed many more LOH events in these same cell lines using

Table 3
Spectra of spontaneous TK⁻ mutations in TK6⁻20C and TK6-E6 cells

Cell line	Mutation frequency	Number of mutants analyzed	Point mutation	Interstitial deletion	Crossing over	Terminal deletion or tranlocation
			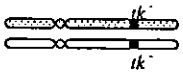	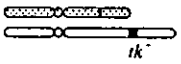	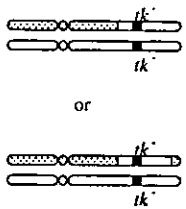	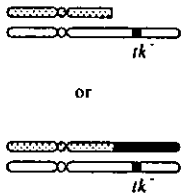
Present study[a]						
TK6-20C	$5.7 \times 10^{-6} \pm 1.3$	110	$2.2 \times 10^{-6} \pm 0.5$	$0.26 \times 10^{-6} \pm 0.13$	$2.9 \times 10^{-6} \pm 0.6$	$0.26 \times 10^{-6} \pm 0.1$
TK6-E6	$32.7 \times 10^{-6} \pm 3.2$	117	$2.2 \times 10^{-6} \pm 0.2$	$0.28 \times 10^{-6} \pm 0.03$	$5.7 \times 10^{-6} \pm 0.3$	$24.5 \times 10^{-6} \pm 1.5$
Previous study[b]						
TK6-20C	$3.8 \times 10^{-6} \pm 1.8$	45	$0.93 \times 10^{-6} \pm 0.24$	$0.51 \times 10^{-6} \pm 0.13$	$1.7 \times 10^{-6} \pm 0.4$	$0.77 \times 10^{-6} \pm 0.2$
TK6-E6	$33.5 \times 10^{-6} \pm 9.8$	16	$1.50 \times 10^{-6} \pm 0.44$	$0.73 \times 10^{-6} \pm 0.21$	$1.5 \times 10^{-6} \pm 0.4$	$30.5 \times 10^{-6} \pm 8.9$

[a] TK⁻ mutants were classified with the length and zygousity (hemizygous or homozygous) of LOH tracts (for TK6-20C, see [28]; for TK6-E6, data are available on request).
[b] Data are from our previous study [19].

Table 4
Distribution of LOH endpoints on chrmosome 17q

LOH marker[a]	Position (Mb)	Interval (Mb)	Nunber of mutants carrying each LOH endpoint[b]						Relative incidence of LOH endpoints/Mb[e]	
			Experiment I[c]		Experiment II[d]		Experiment I + II		20C	E6
			20C	E6	20C	E6	20C	E6		
D17S932	44.77	2.47	0	0	0	0	0	0	<0.6	<0.4
D17S930	47.24	0.77	14	0	0	0	14	0	27.2	<1.3
D17S810	48.01	3.39	0	0	0	0	0	0	<0.3	<0.3
D17S806	51.4	0.86	0	0	0	1	0	1	<0.14	1.7
D17S1827	52.26	1.62	1	1	2	1	3	2	2.7	1.3
D17S588	53.88	2.24	1	2	1	2	2	4	1.3	1.7
D17S788	56.12	3.66	3	4	0	3	3	7	1.2	1.9
D17S1607	59.78	1.87	1	2	1	1	2	3	1.6	1.6
D17S1606	61.65	0.72	0	0	0	2	0	2	<1.2	2.8
D17S1290	62.37	2.28	3	8	0	3	3	11	2	4.8
D17S923	64.65	2.53	2	12	1	7	3	19	1.7	7.2
D17S794	67.18	0.47	0	3	0	2	0	5	<1.7	10.6
D17S948	67.65	1.02	8	6	6	5	14	11	20.5	11
D17S1297	68.67	2.29	0	16	5	6	5	22	3.3	9.6
D17S807	70.96	0.6	1	5	3	2	4	7	10	11.7
D17S1813	71.56	1.43	3	10	0	1	3	11	3.2	7.8
D17S789	72.99	1.53	2	8	0	1	2	9	2	5.9
D17S940	74.52	0.53	9	4	2	1	11	5	31.1	9.4
D17S840	75.05	1.97	0	4	3	2	3	6	2.2	3
D17S1797	76.97	2.24	1	6	0	2	1	8	0.8	3.6
D17S1807	79.21	2.45	2	4	2	1	4	5	2.4	2
D17S785	81.67	0.93	7	6	2	1	9	7	14.5	7.5
D17S937	82.6	0.95	8	3	6	1	14	4	22.1	4.2
tk1										
D17S802	83.55	2.08								
D17S784	85.62	2.71								
D17S928	88.33									
Total			66	104	34	45	100	149		

[a] Microsatellite markers shown by bold letter were those used in multiples PCR with 10 primers.
[b] For interstitial deletions (20C L-12, L-15, L-33 and L-53 of this work, 20C-14 and -25 of previous report), the distal endpoint of LOH tracts were used for mapping.
[c] LOH mutants obtained in this study.
[d] LOH mutants from the previous study [19].
[e] Estimated numbers for TK6-20C were normalized by multiplying the ratio of analyzed LOH mutants of TK6-E6 to TK6-20C (149/100).

a significantly improved LOH detection. Our results appear to indicate that the elevated spontaneous mutation frequency that we observe in p53-abrogated cells is mainly due to increases in the likelihood of specific types of LOH event occurring; these are events that seem to involve either terminal deletions or translocations. By contrast, the frequencies of base substitutions and interstitial deletions (as judged by LOH patterns) appear to have been almost unaffected by the abrogation of p53 status in the cells concerned (Table 3). The frequency of crossing over events was almost not changed by the p53 abrogation in our previous experiment, but enhanced twofold in the present study. This enhancement of crossing over events is, however, much smaller than that of terminal deletions, and can be considered as similar level of changes in the frequencies of base substitutions and interstitial deletions. We could speculate that p53 abrogation does not greatly affect the occurrences of crossing over events. However, it is difficult to conclude that the p53 pro-

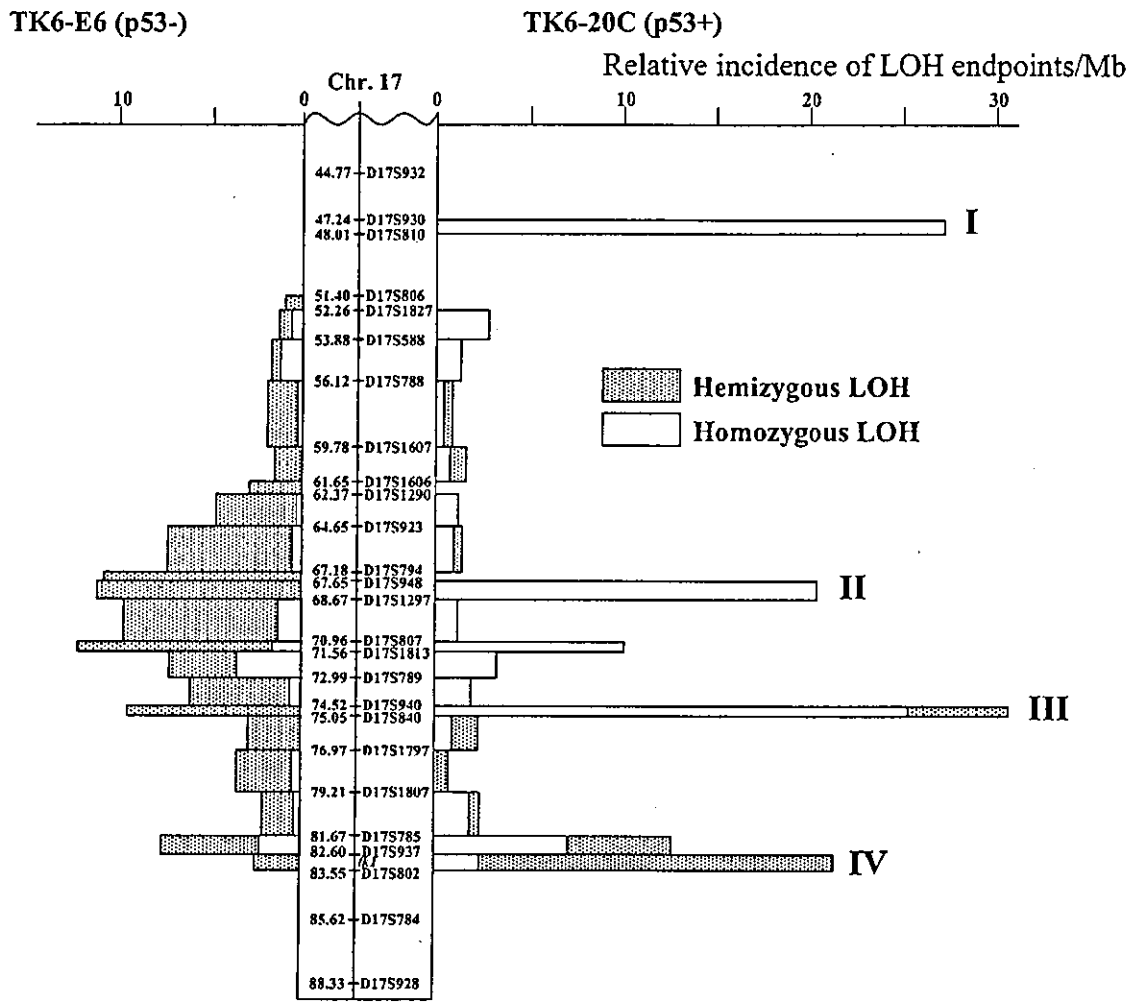

Fig. 3. Mapping of LOH endpoints on the 45 Mb long part of chromosome 17q arm. Distal ends of LOH tracts in 100 and 149 spontaneous LOH mutants, respectively, of TK6-20C and TK6-E6 were mapped on the 45 Mb long chromosome 17q spanning from D17S932 to telomere. LOH status and extent of LOH tracts in those mutants were determined with 26 microsatellite markers as described in Section 2. Relative incidences of LOH endpoints/Mb are shown, on the right for TK6-20C and on the left for TK6-E6, with a genetic map of the 45 Mb long part of chromosome 17q. Homozygous LOHs are shown by open bars and hemizygous LOHs are shown by shadowed bars.

tein is not critically involved in the HR process, because influence of p53 on the quality and quantity needs to be assessed more carefully in separate experiments. Rather, there is good evidence that endogenous levels of p53 may have an antirecombinogenic role in HR in normal human fibroblasts [21]. One must be cautious in interpreting the functions of p53 by looking at individual pathways or systems, however, since the vast p53 data base which has been obtained in studies of many different species-, tissue-, and cell-type specific model systems has on many occasions lead to either confusion or insight with approximately equal probability [22]. For example, in the case of two isogenic human colon cancer cell lines (p53-wild type and p53-null), the rates of numerical and structural chromosomal instabilities and of SCE and HR were essentially unaffected by their p53 status [23], whereas spontaneous chromosome aberrations occurred at several-fold higher rates in p53-null mice than in p53-wild type mice [24].

In eukaryotic cells, DNA DSBs, either of endogenous or exogenous origin, can be repaired by at least two major pathways, NHEJ and HR. NHEJ is the predominant pathway of DSBs repair in mammalian cells, whereas HR appears to be more common in yeast [25]. Interestingly, accumulating evidence suggests that there may be a third pathway of DSB repair in eukaryotic cells, although the mechanism underlying it is elusive as yet [26–28]. In this mechanism, the disappearances of DSBs induced by ionizing radiation in genomic DNA of human cells follow biphasic kinetics. In DNA-PKcs (catalytic subunit of DNA-dependent protein kinase) inactivated human glioma cells, the fast component of repair is severely impaired, but the slow component appears to be able to cope with the majority of the remaining DSBs. In an in vitro assay with calf thymus cell extracts, DSBs induced by ionizing radiation appear to be repaired by either a direct-repeat end joining (DREJ) mechanism, which proceeds even in the absence of DNA-PKcs activity, or a blunt-end joining mechanism (DNA-PKcs-dependent NHEJ) [29]. A recent report indicates that the BRCA1 gene product is capable of assisting microhomology-mediated NHEJ of DSBs, and may also contribute to the maintenance of genomic stability, at least in part by a process involving the Rad50/Mre11/Nbs1 complex [30]. The S-phase checkpoint functions of this complex have recently been found to play an important role in suppressing the spontaneous genome instability which can result from DSB accumulation during DNA replication [31–35].

Although the mechanism underlying the putative third pathway of DSB repair suggested by the above findings has still to be characterized, it appears to have a few common features that hint at a possible mechanism. These are: (i) the rejoining process appears to be widely conserved in eukaryotic cells, from yeast to human, (ii) the rejoining process uses a few of the bases in direct repeats to rejoin broken double-strand DNA, (iii) expression of the pathway may enhance chromosomal aberrations (i.e. genomic instability). This putative DNA-PKcs-independent NHEJ repair system may be responsible for the enhanced LOH events and/or chromosomal instability that we have been observing in p53-abrogated cells TK6-E6. It is therefore important to note that a repair system of this sort may be present in DT 40 cells lacking p53 function. Further points of interest include the fact that p53-null NH32 cells experienced increases in TK^- mutation frequencies that are similar to those we were seeing in p53-abrogated cells TK6-E6 [unpublished data, 36], as well as the recent finding that knockdown of DNA-PKcs by siRNA in NH32 led to almost no change in TK^- mutation frequency [36]. Careful sequencing of the deleted ends and rejoined segments involved in the LOH events that we have been studying should contribute to unveiling the mechanism of this putative NHEJ repair.

The LOH endpoints in p53-wild type cells TK6-20C did not appear to be randomly distributed on the 45 Mb chromosome 17q fragment (Fig. 3). There were four clear peaks of LOH endpoints. Peak I is peculiar in that no LOH endpoints occurred in the regions around this peak in p53-abrogated cells TK6-E6. Given that LOH mutants carrying endpoints at or around this peak position were only ever found in TK6-20C cells in our present study (Table 4), we suspect that this may be at least in part due to subtle differences in the selection procedure for TK^- mutants that we used in conducting these particular experiments. Thus TK^- mutants were selected in TFT medium for 10 days to isolate early mutants and 24 days to isolate late mutants in our most recent experiments, while the selection in our earlier experiments was restricted to 14–16 days period. One possible explanation for these findings is that there may be a growth controlling gene(s) near Peak I which would allow proliferation of TK^- mutants of TK6 cells in TFT medium. Such subtle differences in mutant selection might also account for the lower recovery efficiency of cells showing hemizygous LOH in the TK6-20C cell line that we noted in our earlier experiment (31.1%). Homologous recombination (which tends to be error-free) is a plausible mechanism for the generation of homozygous LOH, while deletion is likely to be a major cause of hemizygous LOH. LOH events mapping at peak IV were mostly hemizygous LOH, while those in other three peaks were mostly homozygous LOH. This suggests that the LOH events with endpoints at peak IV are generated by a different mechanism from the LOH events with endpoints at any of the other peaks. Intriguingly, we found no clear peaks of LOH endpoints in TK6-E6 cells. Instead the endpoints appeared to be very broadly distributed around the positions of two of peaks that were detected in p53-wild type cells, peaks II and III. These results strongly suggest that

the LOH events that we were seeing in p53-abrogated cells and those that we were seeing p53 wild-type cells were generated by different DNA repair mechanisms. The most probable DNA repair mechanism involved in p53-wild type cells is likely to be one in which DSB repair by HR is critical, because crossing over events tend to be the most frequent outcomes in the p53-wild type background (Table 3).

Our overall view of the processes involved in the generation of LOH events is therefore as follows. In proliferating mammalian cells, wild type p53 may arrest the cell cycle at G1 or S, and thereby provide time to repair spontaneous DNA damage, including possible replication errors that might otherwise lead to DSB formation. In p53 deficient cells, this form of cell cycle control is lacking; one possible outcome is that removal of DNA replication associated DSBs by DNA-PKcs-dependent NHEJ would be inhibited or even prevented. In such circumstances, a third, less efficient, DNA-PKcs-independent pathway of NHEJ might play a more important role in DSB repair, and in so doing could account for a marked increase in specific types of LOH events of the sort that we saw occurring in TK6-E6 cells. Here we also could not neglect the possibility that crossing over events and NHEJ events are mutually interactive.

It has recently been shown that the E6 gene product encoded by the human papilloma virus can also abrogate p53-dependent functions by promoting the degradation of p53 [37,38], and so it is not therefore possible for us to rule out the possible involvement of unknown gene products in the enhanced mutator activity that we have been assuming can be directly attributed to p53-abrogation.

Acknowledgements

We thank Dr. Yutaka Ishii of Osaka University and Dr. Elliot Drobetsky of Montreal University for critical reading and comments on the manuscript. This research was supported in part by a Grant-in-Aid from Ministry of Education, Culture, Sports, Science and Technology, and funded in part by "Ground Research for Space Utilization" promoted by National Space Development Agency of Japan and the Japan Space Forum.

References

[1] C. Lengauer, K.W. Kinzler, B. Vogelstein, Genetic instabilities in human cancers, Nature 396 (1998) 643–649.
[2] H.M. Padilla-Nash, W.G. Nash, G.M. Padilla, K.M. Roberson, C.N. Robertson, M. Macville, E. Schrock, T. Ried, Molecular cytogenetic analysis of the bladder carcinoma cell line BK-10 by spectral karyotyping, Genes Chromosomes Cancer 25 (1999) 53–59.
[3] A.G. Knudson, Antioncogenes and human cancer, Proc. Natl. Acad. Sci. USA 90 (1993) 10914–10921.
[4] J.A. Tischfield, Loss of heterozygosity or: how I learned to stop worrying and love mitotic recombination, Am. J. Hum. Genet. 61 (1997) 995–999.
[5] P.K. Gupta, A. Sahota, S.A. Boyadjiev, S. Bye, C. Shao, J.P. O'Neill, T.C. Hunter, R.J. Albertini, P.J. Stambrook, J.A. Tischfield, High frequency in vivo loss of heterozygosity is primarily a consequence of mitotic recombination, Cancer Res. 57 (1997) 1188–1193.
[6] C. Shao, L. Deng, O. Henegariu, L. Liang, N. Raikwar, A. Sahota, P.J. Stambrook, J.A. Tischfield, Mitotic recombination produces the majority of recessive fibroblast variants in heterozygous mice, Proc. Natl. Acad. Sci. USA 96 (1999) 9230–9235.
[7] C. Chen, R.D. Kolodner, Gross chromosomal rearrangements in *Saccharomyces cerevisiae* replication and recombination defective mutants, Nat. Genet. 23 (1999) 81–85.
[8] D.J. Galgoczy, D.P. Toczyski, Checkpoint adaptation precedes spontaneous and damage-induced genomic instability in yeast, Mol. Cell Biol. 21 (2001) 1710–1718.
[9] M. Hiraoka, K. Watanabe, K. Umezu, H. Maki, Spontaneous loss of heterozygosity in diploid *Saccharomyces cerevisiae* cells, Genetics 156 (2000) 1531–1548.
[10] K. Myung, C. Chen, R.D. Kolodner, Multiple pathways cooperate in the suppression of genome instability in *Saccharomyces cerevisiae*, Nature 411 (2001) 1073–1076.
[11] A. Fujimori, A. Tachibana, K. Tatsumi, Allelic losses in mutations at the aprt locus of human lymphoblastoid cells, Mutat. Res. 269 (1992) 55–62.
[12] H.L. Liber, W.G. Thilly, Mutation assay at the thymidine kinase locus in diploid human lymphoblasts, Mutat. Res. 94 (1982) 467–485.
[13] Y. Zhu, P.J. Stambrook, J.A. Tischfield, Loss of heterozygosity: the most frequent cause of recessive phenotype expression at the heterozygous human adenine phosphoribosyltransferase locus, Mol. Carcinog. 8 (1993) 138–144.
[14] A.J. Grosovsky, B.N. Walter, C.R. Giver, DNA-sequence specificity of mutations at the human thymidine kinase locus, Mutat. Res. 289 (1993) 231–243.
[15] C.R. Giver, S.L. Nelson Jr., M.Y. Cha, P. Pongsaensook, A.J. Grosovsky, Mutational spectrum of X-ray induced TK-human cell mutants, Carcinogenesis 16 (1995) 267–275.
[16] M. Honma, L.S. Zhang, M. Hayashi, K. Takeshita, Y. Nakagawa, N. Tanaka, T. Sofuni, Illegitimate recombination leading to allelic loss and unbalanced translocation in p53-mutated human lymphoblastoid cells, Mol. Cell Biol. 17 (1997) 4774–4781.

[17] D.W. Yandell, T.P. Dryja, J.B. Little, Molecular genetic analysis of recessive mutations at a heterozygous autosomal locus in human cells, Mutat. Res. 229 (1990) 89–102.
[18] C.R. Giver, A.J. Grosovsky, Radiation specific patterns of loss of heterozygosity on chromosome 17q, Mutat. Res. 450 (2000) 201–209.
[19] M. Honma, M. Momose, H. Tanabe, H. Sakamoto, Y. Yu, J.B. Little, T. Sofuni, M. Hayashi, Requirement of wild-type p53 protein for maintenance of chromosomal integrity, Mol. Carcinog. 28 (2000) 203–214.
[20] Y. Yu, C.Y. Li, J.B. Little, Abrogation of p53 function by HPV16 E6 gene delays apoptosis and enhances mutagenesis but does not alter radiosensitivity in TK6 human lymphoblast cells, Oncogene 14 (1997) 1661–1667.
[21] S.P. Linke, S. Sengupta, N. Khabie, B.A. Jeffries, S. Buchhop, S. Miska, W. Henning, R. Pedeux, X.W. Wang, L.J. Hofseth, Q. Yang, S.H. Garfield, H.W. Sturzbecher, C.C. Harris, p53 interacts with hRAD51 and hRAD54, and directly modulates homologous recombination, Cancer Res. 63 (2003) 2596–2605.
[22] B. Vogelstein, D. Lane, A.J. Levine, Surfing the p53 network, Nature 408 (2000) 307–310.
[23] F. Bunz, C. Fauth, M.R. Speicher, A. Dutriaux, J.M. Sedivy, K.W. Kinzler, B. Vogelstein, C. Lengauer, Targeted inactivation of p53 in human cells does not result in aneuploidy, Cancer Res. 62 (2002) 1129–1133.
[24] S.D. Bouffler, C.J. Kemp, A. Balmain, R. Cox, Spontaneous and ionizing radiation-induced chromosomal abnormalities in p53-deficient mice, Cancer Res. 55 (1995) 3883–3889.
[25] P.A. Jeggo, DNA breakage and repair, Adv. Genet. 38 (1998) 186–218.
[26] J. Thacker, Repair of ionizing radiation damage in mammalian cells. Alternative pathways and their fidelity, C R Acad. Sci. III 322 (1999) 103–108.
[27] P. Karran, DNA double strand break repair in mammalian cells, Curr. Opin. Genet. Dev. 10 (2000) 144–150.
[28] K.K. Khanna, S.P. Jackson, DNA double-strand breaks: signaling, Nat. Genet. 27 (2001) 247–254.
[29] R.M. Mason, J. Thacker, M.P. Fairman, The joining of non-complementary DNA double-strand breaks by mammalian extracts, Nucleic Acids Res. 24 (1996) 4946–4953.
[30] Q. Zhong, T.G. Boyer, P.L. Chen, W.H. Lee, Deficient nonhomologous end-joining activity in cell-free extracts from Brca1-null fibroblasts, Cancer Res. 62 (2002) 3966–3970.
[31] V. Costanzo, K. Robertson, M. Bibikova, E. Kim, D. Grieco, M. Gottesman, D. Carroll, J. Gautier, Mre11 protein complex prevents double-strand break accumulation during chromosomal DNA replication, Mol. Cell 8 (2001) 137–147.
[32] A. Franchitto, P. Pichierri, Bloom's syndrome protein is required for correct relocalozation of RAD50/MRE11/NBS1 complex after replication fork arrest, J. Cell Biol. (2002) 19–30.
[33] J. Falck, N. Mailand, R.G. Syljuasen, J. Bartek, J. Lukas, The ATM-Chk2-Cdc25A checkpoint pathway guards against radioresistant DNA synthesis, Nature 410 (2001) 842–847.
[34] K. Myung, A. Datta, R.D. Kolodner, Suppression of spontaneous chromosomal rearrangements by S Phase checkpoint functions in *Saccharomyces cerevisiae*, Cell 104 (2001) 329–332.
[35] K. Myung, R.D. Kolodner, Suppression of genome instability by redundant S-phase checkpoint pathways in *Saccharomyces cerevisiae*, Proc. Natl. Acad. Sci. USA 99 (2002) 4500–4507.
[36] Y. Peng, Q. Zhang, H. Nagasawa, R. Okayasu, H.L. Liber, J.S. Bedford, Silencing expression of the catalytic subunit of DNA-dependent protein kinase by small interfering RNA sensitizes human cells for radiation-induced chromosome damage, cell killing, and mutation, Cancer Res. 62 (2002) 6400–6404.
[37] M. Scheffner, B.A. Werness, J.M. Huibregtse, A.J. Levine, P.M. Howley, The E6 oncoprotein encoded by human papillomavirus types 16 and 18 promotes the degradation of p53, Cell 63 (1990) 1129–1136.
[38] T. Crook, J.A. Tidy, K.H. Vousden, Degradation of p53 can be targeted by HPV E6 sequences distinct from those required for p53 binding and trans-activation, Cell 67 (1991) 547–556.

Available online at www.sciencedirect.com
SCIENCE DIRECT
ELSEVIER
Mutation Research 559 (2004) 83–95
Genetic Toxicology and Environmental Mutagenesis
www.elsevier.com/locate/gentox
Community address: www.elsevier.com/locate/mutres

In vivo mutagenicity of benzo[*f*]quinoline, benzo[*h*]quinoline, and 1,7-phenanthroline using the *lacZ* transgenic mice

Katsuya Yamada [a], Takayoshi Suzuki [b], Arihiro Kohara [a,b], Makoto Hayashi [b], Takaharu Mizutani [a], Ken-Ichi Saeki [a,*]

[a] *Graduate School of Pharmaceutical Sciences, Nagoya City University, Tanabedori, Mizuho-ku, Nagoya 467-8603, Japan*
[b] *Division of Genetics and Mutagenesis, National Institute of Health Sciences, 1-18-1 Kamiyoga, Setagaya-ku, Tokyo 158-8501, Japan*

Received 25 September 2003; received in revised form 26 December 2003; accepted 26 December 2003

Abstract

Phenanthrene, a simplest angular polycyclic aromatic hydrocarbon with a bay-region in its molecule, is reported to be non-mutagenic, although most angular (non-linear) polycyclic aromatic hydrocarbons, such as benzo[*a*]pyrene and chrysene, are known to show genotoxicity after metabolic transformation into a bay-region diol epoxide. On the other hand, benzo[*f*]quinoline (BfQ), benzo[*h*]quinoline (BhQ), and 1,7-phenanthroline (1,7-Phe), which are all aza-analogs of phenanthrene, are mutagenic in the Ames test using *Salmonella typhimurium* TA100 in the presence of a rat liver S9 fraction. In this report, we undertook to investigate the in vivo mutagenicity of BfQ, BhQ and 1,7-Phe by an in vivo mutation assay system using the *lacZ* transgenic mouse (Muta™Mouse). BfQ and BhQ only slightly induced mutation in the liver and lung, respectively. BfQ- and BhQ-induced *cII* mutant spectra showed no characteristics compared with that of the control. These results suggest that the in vivo mutagenicities of BfQ and BhQ were equivocal. On the other hand, 1,7-Phe induced a potent mutation in the liver and a weak mutation in the lung. Furthermore 1,7-Phe depressed the G:C to A:T transition and increased the G:C to C:G transversion in the liver like quinoline, a hepatomutagen possessing the partial structure of 1,7-Phe, compared with the spontaneous mutation spectrum. These results suggest that the in vivo mutagenicity of 1,7-Phe might be caused by the same mechanism as that of quinoline, which induced the same mutational spectrum change (G:C to C:G transversion).

Keywords: Tricyclic aza-arene; In vivo mutagenesis assay; Mutation spectrum

1. Introduction

Carcinogenic aza-arenes are widely distributed in the environmental pollutants such as cigarette smoke [1] and urban air [2–4]. Although numerous studies about the in vitro mutagenicity of aza-arenes have been reported, the metabolic activation mechanism of aza-arenes has not yet been elucidated, except for that of heterocyclic amines. Furthermore, there are only a few reports about the in vivo mutagenicity of aza-arenes. We have investigated the in vitro and in vivo mutagenicity of aza-arenes with special attention to their metabolic activation mechanisms. 10-Azabenzo[*a*]pyrene, a carcinogenic aza-analog [5] of benzo[*a*]pyrene, was reported to be as mutagenic as benzo[*a*]pyrene in the Ames test using *Salmonella typhimurium* TA100 in the presence of a rat liver S9 fraction [6–8]. In our previous study,

* Corresponding author. Tel.: +81-52-836-3485; fax: +81-52-834-9309.
E-mail address: saeki@phar.nagoya-cu.ac.jp (K.-I. Saeki).

1383-5718/$ – see front matter © 2004 Elsevier B.V. All rights reserved.
doi:10.1016/j.mrgentox.2003.12.012

Fig. 1. Structures of BfQ, BhQ and 1,7-Phe.

10-azabenzo[*a*]pyrene showed significant mutagenicity only in the liver and colon in an in vivo mutation assay system using the *lacZ* transgenic mouse (Muta^{TM}Mouse) [9]. We have also reported that the total dose of 200 mg/kg (50 mg/kg per day × 4 days) of quinoline, a hepatocarcinogenic [10,11] aza-analog of naphthalene, showed a potent mutagenicity and induced primarily G:C to C:G transversions in the liver of Muta^{TM}Mouse [12–14].

Phenanthrene, a simplest angular polycyclic aromatic hydrocarbon with a bay-region in its molecule, has been reported to be non-mutagenic [15], although most angular (non-linear) polycyclic aromatic hydrocarbons, such as benzo[*a*]pyrene and chrysene, are known to show genotoxicity after metabolic transformation into a bay-region diol epoxide. On the other hand, it was reported that benzo[*f*]quinoline (BfQ) and 1,7-phenanthroline (1,7-Phe) (Fig. 1), which are environmental contaminants and aza-analogs of phenanthrene, were mutagenic in the Ames test using *S. typhimurium* TA100 in the presence of a rat liver S9 fraction [16–18]. Furthermore, benzo[*h*]quinoline (BhQ) (Fig. 1), a positional isomer of BfQ, was reported to be weakly or equivocally mutagenic in *S. typhimurium* TA100 with a rat liver S9 fraction [19,20]. In our previous report, it was suggested that metabolic activation of these tricyclic aza-arenes might take place in the pyridine moiety, like quinoline, to form the ultimate genotoxic form, an enamine epoxide (*N*,d-hydrated a,b-epoxide) (Fig. 2) [18].

In the present study, we undertook to investigate the in vivo mutagenicity of BfQ, BhQ and 1,7-Phe by the in vivo mutation assay system using the *lacZ* transgenic mouse (Muta^{TM}Mouse).

2. Materials and methods

2.1. Materials

BfQ (CAS Registry No. 85-02-9) and BhQ (CAS Registry No. 230-27-3) were purchased from Tokyo Kasei Kogyo Co. Ltd. (Tokyo), 1,7-Phe (CAS Registry No. 230-46-6) from Aldrich, phenyl-β-D-galactoside (P-gal) from Sigma Chemical Co. (St. Louis, MO, USA), proteinase K and olive oil from Wako Pure Chemicals (Osaka), and RNase from Boeringer Mannheim.

2.2. In vivo mutagenesis assay using Muta^{TM}Mouse

2.2.1. Animals and treatments

Seven-week-old male Muta^{TM}Mice, supplied by COVANCE Research Products (PA, USA), were acclimatized for 1 week before use and divided into seven groups of four mice each. BfQ, BhQ, and 1,7-Phe dissolved in olive oil (10 ml/kg body weight) were injected intraperitoneally into two, one, and two groups, respectively, at single doses of 100, 100, and 50 mg/kg, respectively, for four consecutive days. The remaining two groups were given olive oil as the control.

2.2.2. Tissues and DNA isolation

All mice were killed by cervical dislocation 14 days (BfQ-, BhQ-, 1,7-Phe- and olive oil-treated groups) or 56 days (BfQ-, 1,7-Phe- and olive oil-treated groups) after the last injection of a test chemical. The liver, spleen, lung, kidney, and bone marrow were immedi-

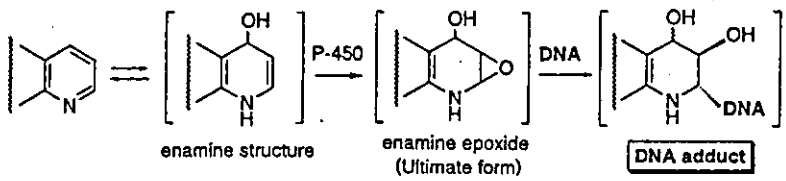

Fig. 2. Proposed metabolic activation pathway for the pyridine moiety (enamine epoxide theory).

ately extirpated, frozen in liquid nitrogen, and stored at −80 °C until DNA extraction. The genomic DNA was extracted from each tissue by the phenol/chloroform method as previously reported [12]. The isolated DNA was precipitated with ethanol, air-dried, and dissolved in an appropriate volume (20–200 μl) of TE-4 buffer (10 mM Tris–HCl at pH 8.0 containing 4 mM EDTA) at room temperature overnight. The DNA solution thus prepared was stored at 4 °C.

2.2.3. In vitro packaging

The lambda gt10/*lacZ* vector was efficiently recovered by the in vitro packaging reactions [21]. Our home-made (HM) packaging extract consisting of a sonic extract (SE) of *Escherichia coli* NM759 and a freeze–thaw lysate (FTL) of *E. coli* BHB2688 was prepared according to the methods of Gunther et al. [22]. As the general procedure for handling the HM extract, approximately 5 μg DNA was mixed with 15 μl of FTL and 30 μl of SE and incubated at 37 °C for 90 min. Then the SE and FTL were combined again and the mixture was incubated for another 90 min. The reaction was terminated by the addition of an appropriate volume of SM buffer (50 mM Tris–HCl at pH 7.5, 10 mM $MgSO_4$, 100 mM NaCl, 0.01% gelatin) and stored at 4 °C. By this procedure, the λgt10 vector was efficiently rescued from genomic DNA to form an infectious phage.

2.2.4. Mutation assays

2.2.4.1. lacZ mutant frequency determination. The positive selection for *lacZ* mutants was performed as previously reported [12,23]. Briefly, the phage solution was absorbed to *E. coli* C (*lac*$^-$ *galE*$^-$) at room temperature for 20–30 min. For titration, an aliquot of the phage-*E. coli* solution was mixed with LB top agar (containing 10 mM $MgSO_4$) and plated onto dishes containing bottom agar. The remaining phage-*E. coli* solution was mixed with LB top agar containing phenyl-β-D-galactoside (P-gal) (3 mg/ml) and plated as described above. The mutant frequency (MF) was calculated by the following formula:

$$\text{mutant frequency} = \left(\frac{\text{total number of plaques on selection plates}}{\text{total number of plaques on titer plates}}\right) \times \text{dilution factor.}$$

The significance of differences in the mutant frequency between the treated and control groups was analyzed by using Student's *t*-test.

2.2.4.2. cII mutant frequency determination. We also examined the mutagenicity in the lambda *cII* gene integrated as a lambda vector gene, which serves as another selective marker as reported previously in the *lacI* transgenic BigBlue mouse [24]. The positive

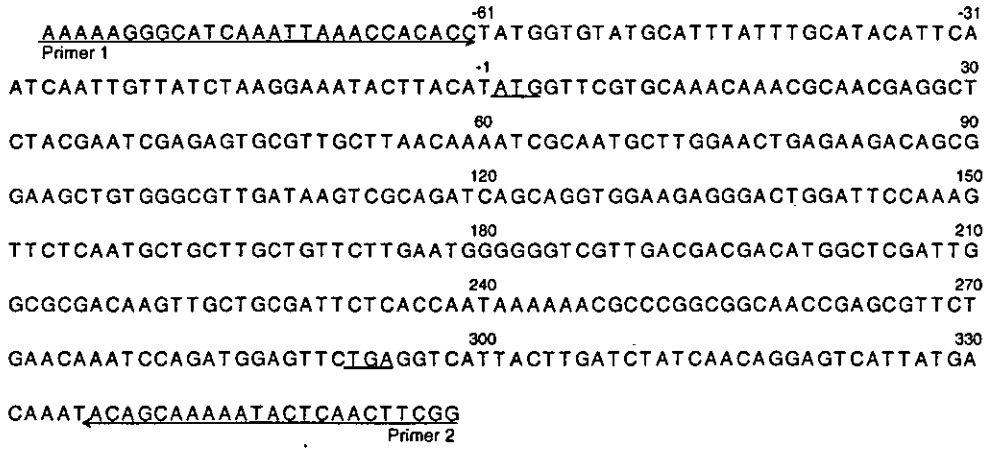

Fig. 3. Sequence map of the *cII* gene. The primers, used for PCR amplification and sequencing, are shown by arrows. The PCR gives 446 bp products that involve the entire (294 bp) *cII* gene. Initiation and stop codons are underlined.

Table 1
Mutant frequencies induced by BfQ, BhQ and 1,7-Phe in five organs of Muta™Mouse for the expression time of 14 days

Tissue	Treatment	*lacZ* assay				*cII* assay			
		Individual animal data			Average ± S.D.	Individual animal data			Average ± S.D.
		No. of phages analyzed	No. of mutants	MF × 10^5	MF × 10^5	No. of phages analyzed	No. of mutants	MF × 10^5	MF × 10^5
Liver	Control (olive oil)	1120000	106	9.5	7.0 ± 1.6	449400	12	2.7	2.1 ± 0.6
		816000	59	7.2		938400	24	2.6	
		1198000	73	6.1		764400	11	1.4	
		791500	41	5.2		699000	11	1.6	
	BfQ	634500	32	5.0	9.6 ± 3.1	804600	12	1.5	3.8 ± 1.6
		590000	51	8.6		662400	35	5.3	
		158500	20	12.6		426300	23	5.4	
		221500	27	12.2		883200	28	3.2	
	BhQ	442000	29	6.6	5.9 ± 1.1	1188000	53	4.5	2.6 ± 1.1
		677000	39	5.8		1134600	21	1.9	
		257500	11	4.3		671700	17	2.5	
		645500	46	7.1		1011000	15	1.5	
	1,7-Phe	272000	41	15.1	15.9 ± 0.5**	813600	44	5.4	4.1 ± 0.8*
		183000	30	16.4		562800	19	3.4	
		263000	43	16.3		720000	25	3.5	
		184000	29	15.8		606000	25	4.1	
Spleen	Control (olive oil)	855500	116	13.6	7.3 ± 3.6	623100	12	1.9	2.4 ± 0.3
		533000	29	5.4		1502400	41	2.7	
		446500	25	5.6		546900	15	2.7	
		461000	22	4.8		569400	13	2.3	
	BfQ	210500	13	6.2	6.1 ± 0.6	2098200	25	1.2	3.5 ± 2.8
		244500	16	6.5		441000	13	2.9	
		403000	27	6.7		785400	65	8.3	
		256500	13	5.1		786600	13	1.7	
	BhQ	297000	12	4.0	6.5 ± 1.6	277800	10	3.6	2.9 ± 0.6
		354500	25	7.1		828300	22	2.7	
		396500	26	6.6		946200	31	3.3	
		544000	46	8.5		1608600	34	2.1	
	1,7-Phe	426500	34	8.0	7.0 ± 1.0	967200	20	2.1	2.4 ± 0.7
		502500	27	5.4		1023000	24	2.3	
		320000	24	7.5		1026900	16	1.6	
		462500	34	7.4		905400	32	3.5	
Lung	Control (olive oil)	1539500	127	8.2	6.0 ± 1.3	1027800	21	2.0	2.1 ± 0.4
		1111500	60	5.4		738000	21	2.8	
		678000	35	5.2		1142700	20	1.8	
		1473000	76	5.2		831600	15	1.8	
	BfQ	553000	39	7.1	6.0 ± 0.6	1107600	18	1.6	2.6 ± 0.6
		332000	18	5.4		903300	22	2.4	
		353000	21	5.9		1124700	36	3.2	
		266000	15	5.6		445200	14	3.1	
	BhQ	401500	51	12.7	10.8 ± 2.4*	1705500	37	2.2	3.5 ± 1.0
		481500	54	11.2		1071000	33	3.1	
		572500	72	12.6		2403000	99	4.1	
		372000	25	6.7		2083200	98	4.7	

Table 1 (*Continued*)

Tissue	Treatment	*lacZ* assay				*cII* assay			
		Individual animal data			Average ± S.D.	Individual animal data			Average ± S.D.
		No. of phages analyzed	No. of mutants	MF × 10^5	MF × 10^5	No. of phages analyzed	No. of mutants	MF × 10^5	MF × 10^5
	1,7-Phe	335500	29	8.6	10.3 ± 1.9*	1103400	26	2.4	2.9 ± 0.5
		351000	46	13.1		1012200	27	2.7	
		244500	27	11.0		909600	34	3.7	
		211000	18	8.5		892200	26	2.9	
Kidney	Control (olive oil)	219500	15	6.8	6.8 ± 1.4	551100	21	3.8	2.7 ± 1.0
		190000	17	8.9		426600	16	3.8	
		349500	17	4.9		588000	11	1.9	
		301000	20	6.6		771000	12	1.6	
	BfQ	682500	46	6.7	7.4 ± 1.1	1035000	25	2.4	3.9 ± 0.9
		550500	51	9.3		825000	36	4.4	
		474000	33	7.0		649800	30	4.6	
		484000	32	6.6		1599000	66	4.1	
	BhQ	920500	55	6.0	7.4 ± 1.2	1323600	26	2.0	2.2 ± 0.5
		622000	51	8.2		945000	27	2.9	
		113000	10	8.8		1408800	23	1.6	
		244500	16	6.5		1018200	23	2.3	
	1,7-Phe	486500	30	6.2	6.8 ± 0.5	814800	15	1.8	3.3 ± 1.6
		558000	38	6.8		660300	40	6.1	
		177000	12	6.8		520200	13	2.5	
		319500	24	7.5		1664700	48	2.9	
Bone marrow	Control (olive oil)	311000	32	10.3	7.1 ± 3.0	644100	14	2.2	1.3 ± 0.6
		465000	27	5.8		1041000	16	1.5	
		70500	2	2.8		111300	1	0.9	
		96500	9	9.3		154500	1	0.6	
	BfQ	325500	17	5.2	6.4 ± 0.9	1075200	16	1.5	2.6 ± 0.9
		256500	17	6.6		528000	12	2.3	
		326000	25	7.7		572100	22	3.8	
		708500	44	6.2		1144800	32	2.8	
	BhQ	257000	13	5.1	5.7 ± 0.5	1757100	20	1.1	1.7 ± 0.4
		617000	38	6.2		1349400	24	1.8	
		683000	41	6.0		1040400	22	2.1	
	1,7-Phe	502500	24	4.8	4.7 ± 0.5	963600	12	1.2	1.6 ± 0.6
		397500	19	4.8		962400	11	1.1	
		622000	33	5.3		1341000	21	1.6	
		332000	13	3.9		916900	24	2.6	

* Significantly different from the control group, $P < 0.05$.
** Significantly different from the control group, $P < 0.01$.

selection for *cII* mutants was performed according to the method of Jakubczak et al. [24] with slight modification as previously reported [14]. Briefly, the phage solution was absorbed to *E. coli* G1225 (*hfl*$^-$) at room temperature for 20–30 min. For titration, an appropriately diluted phage-*E. coli* solution was mixed with LB top agar (containing 10 mM $MgSO_4$), plated onto dishes containing bottom agar, and incubated for 24 h at 37 °C. The remaining phage-*E. coli* solution was mixed with LB top agar and plated onto dishes con-

Table 2
Mutant frequencies induced by BfQ and 1,7-Phe in five organs of Muta™Mouse for the expression time of 56 days

Tissue	Treatment	*lacZ* assay				*cII* assay			
		Individual animal data			Average ± S.D.	Individual animal data			Average ± S.D.
		No. of phages analyzed	No. of mutants	MF × 10^5	MF × 10^5	No. of phages analyzed	No. of mutants	MF × 10^5	MF × 10^5
Liver	Control (olive oil)	246500	21	8.5	7.9 ± 1.3	960700	18	1.9	1.7 ± 0.2
		168500	12	7.1		1161000	21	1.8	
		636500	39	6.1		3351900	65	1.9	
		155500	15	9.6		1978900	27	1.4	
	BfQ	259000	24	9.3	11.5 ± 2.8	543600	14	2.6	2.4 ± 0.2**
		367000	35	9.5		2746500	60	2.2	
		714000	116	16.2		3693000	97	2.6	
		180500	20	11.1		2490600	57	2.3	
	1,7-Phe	653000	63	9.6	14.8 ± 3.7*	1468200	64	4.4	4.8 ± 1.2**
		266500	35	13.1		1140000	36	3.2	
		497000	94	18.9		4469100	286	6.4	
		126000	22	17.5		306600	16	5.2	
Spleen	Control (olive oil)	608500	47	7.7	7.8 ± 0.4	1825800	53	2.9	2.9 ± 0.6
		347500	26	7.5		1304400	48	3.7	
		355500	30	8.4		1224600	36	2.9	
		389500	29	7.4		1106400	22	2.0	
	BfQ	440000	38	8.6	8.4 ± 0.3	2245800	32	1.4	3.3 ± 2.5
		242500	21	8.7		860400	14	1.6	
		354000	30	8.5		1090800	83	7.6	
		460500	36	7.8		946200	24	2.5	
	1,7-Phe	567000	81	14.3	10.0 ± 2.5	1022400	22	2.2	2.2 ± 0.04
		231500	18	7.8		976800	22	2.3	
		336000	29	8.6		1059000	23	2.2	
		253500	24	9.5		865800	19	2.2	
Lung	Control (olive oil)	390500	25	6.4	7.9 ± 1.9	657600	13	2.0	3.1 ± 0.9
		218500	21	9.6		1230600	30	2.4	
		558500	32	5.7		936000	35	3.7	
		474500	47	9.9		928800	38	4.1	
	BfQ	332500	26	7.8	7.2 ± 1.2	742200	19	2.6	3.7 ± 1.9
		554500	43	7.8		1035000	25	2.4	
		476000	39	8.2		839400	59	7.0	
		386000	20	5.2		651000	17	2.6	
	1,7-Phe	731500	56	7.7	7.7 ± 0.9	1365600	25	1.8	3.0 ± 0.9
		412000	32	7.8		728400	29	4.0	
		494500	44	8.9		966600	26	2.7	
		519000	33	6.4		946800	35	3.7	
Kidney	Control (olive oil)	442500	26	5.9	8.2 ± 2.4	1874400	64	3.4	2.5 ± 0.6
		217000	26	12.0		2313600	43	1.9	
		383000	25	6.5		1139400	25	2.2	
		596500	50	8.4		1437600	39	2.7	
	BfQ	552500	41	7.4	7.1 ± 1.0	1629600	60	3.7	2.9 ± 0.7
		479000	39	8.1		1360800	33	2.4	
		774500	56	7.2		1446000	50	3.5	
		698500	38	5.4		1277400	27	2.1	

Table 2 (*Continued*)

Tissue	Treatment	*lacZ* assay				*cII* assay			
		Individual animal data			Average ± S.D.	Individual animal data			Average ± S.D.
		No. of phages analyzed	No. of mutants	MF × 10^5	MF × 10^5	No. of phages analyzed	No. of mutants	MF × 10^5	MF × 10^5
	1,7-Phe	299500	19	6.3	7.3 ± 1.1	1201800	26	2.2	2.2 ± 0.3
		567500	50	8.8		1393200	35	2.5	
		877500	70	8.0		1409400	35	2.5	
		513500	32	6.2		1060200	19	1.8	
Bone marrow	Control (olive oil)	607500	43	7.1	7.9 ± 1.2	1334700	21	1.6	1.9 ± 0.4
		829000	57	6.9		1204800	25	2.1	
		924500	70	7.6		1441800	23	1.6	
		605500	60	9.9		1184400	30	2.5	
	BfQ	429000	26	6.1	6.9 ± 2.1	1703400	19	1.1	3.9 ± 4.1
		661500	69	10.4		1287600	15	1.2	
		893000	47	5.3		1256400	136	10.8	
		791500	45	5.7		1249200	29	2.3	
	1,7-Phe	605500	92	15.2	9.0 ± 3.8	1206600	13	1.1	1.5 ± 0.3
		447500	39	8.7		1700400	22	1.3	
		507000	30	5.9		876000	14	1.6	
		1188000	71	6.0		1444200	28	1.9	

* Significantly different from the control group, $P < 0.05$.
** Significantly different from the control group, $P < 0.01$.

taining bottom agar. The plates were incubated for 48 h at 25 °C for selection of *cII* mutants. The wild type phage, recovered from Muta™Mouse, has a cI^- phenotype, which permits plaque formation with the hfl^- strain at 37 °C but not at 25 °C. The mutant frequency was calculated by the following formula:

$$\text{mutant frequency} = \left(\frac{\text{total number of plaques on selection plates}}{\text{total number of plaques on titer plates}}\right) \times \text{dilution factor.}$$

The significance of differences in the mutant frequency between the treated and control groups was analyzed by using Student's *t*-test.

2.2.5. Sequencing of mutants

The entire lambda *cII* region was amplified directly from mutant plaques by the use of Taq DNA polymerase (Takara Shuzo, Tokyo, Japan) with primers P1; 5′-AAAAAGGGCATCAAATTAAACC-3′, and P2; 5′-CCGAAGTTGAGTATTTTTGCTGT-3′ as previously reported [14] (Fig. 3). A 446 bp PCR product was purified with a microspin column (Amersham Pharmacia, Tokyo, Japan) and then used for a sequencing reaction with the Ampli Taq cycle sequencing kit (PE Biosystems, Tokyo, Japan) using the primer P1. The reaction product was purified by ethanol precipitation and analyzed with the ABI PRISM™ 310 genetic analyzer (PE Biosystems).

3. Results

3.1. Mutant frequency of BfQ, BhQ, and 1,7-Phe

BfQ, BhQ, and 1,7-Phe (Fig. 1) were tested for in vivo mutagenicity using *lacZ* transgenic mice (Muta™Mice). The mutant frequencies observed in the DNA preparations extracted from the five organs are shown in Tables 1 and 2. Over 10 mutant plaques were analyzed in most organs. For the bone marrow in Table 1, the mutant frequency of one animal in the BhQ-treated group was missing and the number of mutants in two animals in the control group was insufficient because the isolated DNA was not enough

to be analyzed. The spontaneous mutant frequencies observed in the control group were similar for the five organs in both *lacZ* and *cII* assays regardless of the expression time (14 or 56 days), the rate ranging from 6.0 to 8.2 × 10^{-5} and from 1.3 to 3.1 × 10^{-5}, respectively. These results were similar to those of our previous studies [9,12–14].

Table 1 shows mutant frequencies with the test compounds in the five organs 14 days after the last injection. BfQ slightly, but not significantly, increased the mutant frequency in the liver in both assays. On the other hand, BhQ significantly increased the mutant frequency in the lung in the *lacZ* assay. 1,7-Phe significantly increased the mutant frequency in the liver in both assays and in the lung in the *lacZ* assay.

Mutant frequencies observed in the DNA preparations extracted from the five organs 56 days after the last injection are shown in Table 2. BfQ significantly increased the mutant frequency in the liver in the *cII* assay, whereas the mutant frequency in the *lacZ* assay was slightly, but not significantly, increased. 1,7-Phe significantly increased the mutant frequency in the liver in both assays like the results obtained 14 days

Table 3
Sequences of *cII* mutations in the liver of BfQ-treated Muta™Mouse for the expression time of 14 days

Mutant no.	Position	Mutation	Sequence	Amino acid change
A1	113	C to T	AAG TCG CAG	Ser to Leu
A2	99–100	GG to TT	GTG GGC GTT	Gly to Cys
A3	107	A to C	GTT GAT AAG	Asp to Ala
A4	57	C to G	CTT AAC AAA	Asn to Lys
A5	214	C to T	GCG CGA CAA	Arg to Stop
A6	181	G to T	TGG GGG GTC	Gly to Trp
A7	34	C to T	CTA CGA ATC	Arg to Stop
A8	103	G to A	GGC GTT GAT	Val to Ile
A9	196	G to T	GAC GAC ATG	Asp to Tyr
A10	129	G to C	AGG TGG AAG	Trp to Cys
A11	34	C to T	CTA CGA ATC	Arg to Stop
A12	25	G to A	AAC GAG GCT	Glu to Lys
A13	241–246	−A	AAA AAA CGC	Frameshift
A14	179–184	−G	TGG GGG GTC	Frameshift
A15	57	C to A	CTT AAC AAA	Asn to Lys
A16	35	G to T	CTA CGA ATC	Arg to Leu
A17	179–184	+G	TGG GGG GTC	Frameshift
A18	90–91	GG to TT	GCG GAA GCT	Glu to Stop
A19	94	G to T	GAA GCT GTG	Ala to Ser
A20	115	C to T	TCG CAG ATC	Gln to Stop
A21	193	G to A	GAC GAC GAC	Asp to Asn
A22	64	G to A	ATC GCA ATG	Ala to Thr
A23	103	G to A	GGC GTT GAT	Val to Ile
A24	104	T to C	GGC GTT GAT	Val to Ala
A25	89	C to T	ACA GCG GAA	Ala to Val
A26[a]	64	G to A	ATC GCA ATG	Ala to Thr
A27	175	G to T	CTT GAA TGG	Glu to Stop
A28	25	G to A	AAC GAG GCT	Glu to Lys
A29	34	C to T	CTA CGA ATC	Arg to Stop
A30	100	G to A	GTG GGC GTT	Gly to Ser
A31	62	T to C	AAA ATC GCA	Ile to Thr
A32[a]	25	G to A	AAC GAG GCT	Glu to Lys
A33	196	G to A	GAC GAC ATG	Asp to Asn
A34	179–184	−G	TGG GGG GTC	Frameshift
A35	115	C to A	TCG CAG ATC	Gln to Lys
A36	134	G to C	AAG AGG GAC	Arg to Thr

[a] Ascribable to the same mutation obtained in an identical mouse.

after the last injection. 1,7-Phe did not increase the mutant frequency in the lung for the expression time of 56 days.

3.2. Mutation spectra of BfQ, BhQ, and 1,7-Phe-induced mutations

A total of 36 BfQ-induced mutants in the liver for the expression time of 14 days, 37 BhQ-induced mutants in the lung for 14 days, and 43 1,7-Phe-induced mutants in the liver for 56 days were subjected to sequence analysis. The mutations are characterized in Tables 3–5, and summarized in Table 6. In Table 6, the same mutations in an identical mouse were treated as single events. The data of the spontaneous mutations are from our previous report [9].

1,7-Phe-induced mutations consisted mainly of base substitutions (36/39); G:C to A:T transitions (15/39) and G:C to C:G transversions (10/39) predominated. Compared with the spontaneous mutation spectrum, G:C to A:T transitions decreased and G:C to C:G transversions increased in the mutations by

Table 4
Sequences of *cII* mutations in the lung of BhQ-treated Muta™Mouse for the expression time of 14 days

Mutant no.	Position	Mutation	Sequence	Amino acid change
B1	196	G to A	GAC GAC ATG	Asp to Asn
B2	179–184	+G	TGG GGG GTC	Frameshift
B3	149	A to T	CCA AAG TTC	Lys to Met
B4	241–246	−A	AAA AAA CGC	Frameshift
B5	34	C to T	CTA CGA ATC	Arg to Stop
B6	113	C to T	AAG TCG CAG	Ser to Leu
B7	215	G to T	GCG CGA CAA	Arg to Leu
B8[a]	34	C to T	CTA CGA ATC	Arg to Stop
B9	166	G to C	CTT GCT GTT	Ala to Pro
B10	25	G to A	AAC GAG GCT	Glu to Lys
B11	34	C to T	CTA CGA ATC	Arg to Stop
B12	62	T to C	AAA ATC GCA	Ile to Thr
B13[a]	34	C to T	CTA CGA ATC	Arg to Stop
B14	233	T to C	ATT CTC ACC	Leu to Pro
B15	40	G to A	ATC GAG AGT	Glu to Lys
B16	212	C to T	TTG GCG CGA	Ala to Val
B17[a]	212	C to T	TTG GCG CGA	Ala to Val
B18	113	C to T	AAG TCG CAG	Ser to Leu
B19	46	G to C	AGT GCG TTG	Ala to Pro
B20	179–184	+G	TGG GGG GTC	Frameshift
B21	89	C to T	ACA GCG GAA	Ala to Val
B22	196	G to A	GAC GAC ATG	Asp to Asn
B23	190–198	−GAC	GAC GAC GAC	Frameshift
B24	34	C to T	CTA CGA ATC	Arg to Stop
B25	205	C to T	GCT CGA TTG	Arg to Stop
B26	179–184	−G	TGG GGG GTC	Frameshift
B27	122	G to T	ATC AGC AGG	Ser to Ile
B28	28	G to A	GAG GCT CTA	Ala to Thr
B29	52	C to G	TTG CTT AAC	Leu to Val
B30	197	A to G	GAC GAC ATG	Asp to Gly
B31	212	C to T	TTG GCG CGA	Ala to Val
B32	91	G to T	GCG GAA GCT	Glu to Stop
B33	205	C to T	GCT CGA TTG	Arg to Stop
B34	40	G to A	ATC GAG AGT	Glu to Lys
B35	34	C to T	CTA CGA ATC	Arg to Stop
B36[a]	40	G to A	ATC GAG AGT	Glu to Lys
B37	89	C to T	ACA GCG GAA	Ala to Val

[a] Ascribable to the same mutation obtained in an identical mouse.

Table 5
Sequences of *cII* mutations in the liver of 1,7-Phe-treated Muta™Mouse for the expression time of 56 days

Mutant no.	Position	Mutation	Sequence	Amino acid change
C1	113	C to T	AAG TCG CAG	Ser to Leu
C2	212	C to T	TTG GCG CGA	Ala to Val
C3	125	G to C	AGC AGG TGG	Arg to Thr
C4	196	G to A	GAC GAC ATG	Asp to Asn
C5	40	G to A	ATC GAG AGT	Glu to Lys
C6[a]	212	C to T	TTG GCG CGA	Ala to Val
C7	46	G to C	AGT GCG TTG	Ala to Pro
C8	94	G to C	GAA GCT GTG	Ala to Pro
C9	134	G to T	AAG AGG GAC	Arg to Met
C10	163	C to T	COG CTT GCT	Leu to Phe
C11	34	C to T	CTA CGA ATC	Arg to Stop
C12	179–240	−62 bp		Frameshift
C13	193	G to A	GAC GAC GAC	Asp to Asn
C14	65	C to T	ATC GCA ATG	Ala to Val
C15	164–165	−T	CTT GCT GTT	Frameshift
	166	G to A		
C16	1	A to G	cat ATG GTT	Met to Val
C17	224	C to A	GTT GCT GCG	Ala to Asp
C18	196	G to A	GAC GAC ATG	Asp to Asn
C19	150	G to T	CCA AAG TTC	Lys to Asn
C20	113	C to T	AAG TCG CAG	Ser to Leu
C21[a]	150	G to T	CCA AAG TTC	Lys to Asn
C22	129	G to A	AGG TGG AAG	Trp to Stop
C23	37	A to T	CGA ATC GAG	Ile to Phe
C24	140–141	GG to CT	GAC TGG ATT	Trp to Ser
C25	89	C to A	ACA GCG GAA	Ala to Glu
C26	34	C to T	CTA CGA ATC	Arg to Stop
C27	212	C to T	TTG GCG CGA	Ala to Val
C28	233	T to C	ATT CTC ACC	Leu to Pro
C29	28	G to C	GAG GCT CTA	Ala to Pro
C30	95	C to A	GAA GCT GTG	Ala to Asp
C31	89	C to G	ACA GCG GAA	Ala to Gly
C32	100	G to C	GTG GGC GTT	Gly to Arg
C33	25	G to T	AAC GAG GCT	Glu to Stop
C34	39	C to G	CGA ATC GAG	Ile to Met
C35	103	G to C	GGC GTT GAT	Val to Leu
C36	212	C to T	TTG GCG CGA	Ala to Val
C37	64	G to A	ATC GCA ATG	Ala to Thr
C38	193	G to T	GAC GAC GAC	Asp to Tyr
C39	95	C to A	GAA GCT GTG	Ala to Asp
C40	74	G to C	CTT GGA ACT	Gly to Ala
C41	120	C to G	CAG ATC AGC	Ile to Met
C42[a]	39	C to G	CGA ATC GAG	Ile to Met
C43[a]	64	G to A	ATC GCA ATG	Ala to Thr

[a] Ascribable to the same mutation obtained in an identical mouse.

1,7-Phe. On the other hand, BfQ and BhQ-induced *cII* mutant spectra showed no characteristics compared with that of the control and consisted mainly of G:C to A:T transitions (15/34 and 18/33, respectively).

4. Discussion

In this study, we attempted to investigate the in vivo mutagenicity of three tricyclic aza-arenes, BfQ, BhQ, and 1,7-Phe. They were injected daily for 4 days

Table 6
Summary of *cII* mutation spectra in Muta™Mouse

Mutation class	Control[a] (%)	BfQ[b] (%)	BhQ[c] (%)	1,7-Phe[b] (%)
Total	32 (100)	34 (100)	33 (100)	39 (100)
Base substitution	28 (88)	28 (82)	28 (85)	36 (92)
Transitions				
GC to AT	18 (56)	15 (44)	18 (55)	15 (38)
AT to GC	1 (3)	2 (6)	3 (9)	2 (5)
Transversions				
AT to TA	3 (9)	0 (0)	1 (3)	1 (3)
AT to CG	0 (0)	1 (3)	0 (0)	1 (3)
GC to TA	5 (16)	7 (20)	3 (9)	7 (18)
GC to CG	1 (3)	3 (9)	3 (9)	10 (26)
−1 frameshifts	1 (3)	3 (9)	2 (6)	0 (0)
+1 frameshifts	2 (6)	1 (3)	2 (6)	0 (0)
Deletion	0 (0)	0 (0)	1 (3)	1 (3)
Insertion	0 (0)	0 (0)	0 (0)	0 (0)
Complex	1 (3)	2 (6)	0 (0)	2 (5)

The same mutations from an identical mouse were counted as single events.
[a] The data of the spontaneous mutations are from our previous report [9].
[b] Mutant plaques from the liver.
[c] Mutant plaques from the lung.

into Muta™Mice at the total doses of 400, 400, and 200 mg/kg intraperitoneally, respectively, based on their tolerance doses determined in preliminary tests. Although these aza-analogs of phenanthrene were weak mutagens in Muta™Mouse, different effects on the target organ specificity and mutant spectrum were observed depending on the N-substituted position.

BfQ increased the mutant frequency in the liver for the expression times of both 14 and 56 days. On the other hand, BhQ increased mutagenicity in the lung, but not in the liver. BfQ has a nitrogen atom in the bay-region and BhQ in the non-bay-region. Therefore, the difference in the nitrogen position in the benzoquinoline molecule might alter the target organ. Quinoline has previously shown a potent in vivo mutagenicity in Muta™Mice [12–14]. These results suggest that in vivo mutagenicity is decreased by the benzene-ring fusion on the quinoline moiety. 1,7-Phe significantly increased mutagenicity in the liver for the expression times of both 14 and 56 days and in the lung for the expression time of 14 days. It may be suggested that 1,7-Phe induced mutation both in the liver and lung because 1,7-Phe has a nitrogen atom in both the bay- and non-bay-regions. Our previous data indicated that metabolic activation of these phenanthrene aza-analogs might take place in the pyridine moiety [18] (Fig. 2). LaVoie and co-workers reported that BfQ might be converted to the ultimate form not only by the bay-region mechanism but also by another mechanism [17], supporting our opinion.

With regard to the suitable expression time in the evaluation of in vivo mutagenicity, different tendencies were observed between the mutagenesis of 1,7-Phe in the liver and that in the lung. 1,7-Phe showed similar mutagenicities in the liver after the expression time of both 14 and 56 days. However, in the lung, 1,7-Phe increased the mutant frequency in the lung after the expression time of 14 days, but not after 56 days. Sun and Heddle reported that mutation by ethylnitrosourea in the liver was more firmly established after about 40 days post-treatment than after 20 days [25]. It seems that an appropriate expression time may be necessary to evaluate the in vivo mutagenicity of chemicals in each organ.

1,7-Phe also depressed the G:C to A:T transition and increased the G:C to C:G transversion like quinoline [14], a hepatomutagen possessing the partial structure of 1,7-Phe, compared with the spontaneous mutation spectrum. Therefore it may be suggested that the increase of G:C to C:G transversions might be a common feature of the quinoline-type metabolic activation in aza-arenes.

Although a major question to be answered is how the position of the nitrogen atom is responsible for the differences in mutagenicity between these tricyclic aza-arenes, the present data suggest that the position of the nitrogen atom in the polycyclic aromatic ring might influence in vivo mutagenicity with respect to the target organ specificity and mutational pattern.

Acknowledgements

We thank Dr. T. Nohmi for his kind gifts of *E. coli* NM759 and BHB2688, and Dr. K. Masumura for his technical guidance in making packaging extracts. This research is supported in part by the grant from the Ministry of Environment, Japan.

References

[1] I. Schmeltz, D. Hoffmann, Nitrogen-containing compounds in tobacco and tobacco smoke, Chem. Rev. 77 (1977) 295–311.
[2] M. Dong, D.C. Locke, D. Hoffmann, Characterization of aza-arenes in basic organic portion of suspended particulate matter, Environ. Sci. Technol. 11 (1977) 612–618.
[3] C.R. Engel, E. Sawicki, A superior thin-layer chromatographic procedure for the separation of aza arenes and its application to air pollution, J. Chromatogr. 31 (1967) 109–119.
[4] D. Brocco, A. Cimmino, M. Possanzini, Determination of azaheterocyclic compounds in atmospheric dust by a combination of thin-layer and gas chromatography, J. Chromatogr. 84 (1973) 371–377.
[5] A. Lacassagne, N.P. Buu-Hoi, F. Zajdela, P. Mabille, Carcinogenic activity of some isosteric nitrogenous pentacyclic hydrocarbon carcinogens, Compt. Rend. 258 (1964) 3387–3389.
[6] Y. Kitahara, H. Okuda, K. Shudo, T. Okamoto, M. Nagao, Y. Seino, T. Sugimura, Synthesis and mutagenicity of 10-azabenzo[*a*]pyrene-4,5-oxide and other pentacyclic aza-arene oxides, Chem. Pharm. Bull. (Tokyo) 26 (1978) 1950–1953.
[7] H. Okuda, Y. Kitahara, K. Shudo, T. Okamoto, Identification of an ultimate mutagen of 10-azabenzo[*a*]pyrene: microsomal oxidation of 10-azabenzo[*a*]pyrene to 10-azabenzo[*a*]pyrene-4,5-oxide, Chem. Pharm. Bull. (Tokyo) 27 (1979) 2547–2549.
[8] C.H. Ho, B.R. Clark, M.R. Guerin, B.D. Barkenbus, T.K. Rao, J.L. Epler, Analytical and biological analysis of test materials from the synthetic fuel technologies, Mutat. Res. 85 (1981) 335–345.
[9] K. Yamada, T. Suzuki, A. Kohara, M. Hayashi, A. Hakura, T. Mizutani, K.I. Saeki, Effect of 10-aza-substitution on benzo[*a*]pyrene mutagenicity in both in vivo and in vitro, Mutat. Res. 521 (2002) 187–200.
[10] K. Hirao, Y. Shinohara, H. Tsuda, S. Fukushima, M. Takahashi, Carcinogenic activity of quinoline on rat liver, Cancer Res. 36 (1976) 329–335.
[11] Y. Shinohara, T. Ogiso, M. Hananouchi, K. Nakanishi, T. Yoshimura, N. Ito, Effect of various factors on the induction of liver tumors in animals by quinoline, Jpn. J. Cancer Res. 68 (1977) 785–796.
[12] T. Suzuki, Y. Miyata, K.I. Saeki, Y. Kawazoe, M. Hayashi, T. Sofuni, In vivo mutagenesis by the hepatocarcinogen quinoline in the *lacZ* transgenic mouse: evidence for its in vivo genotoxicity, Mutat. Res. 412 (1998) 161–166.
[13] Y. Miyata, K.I. Saeki, Y. Kawazoe, M. Hayashi, T. Sofuni, T. Suzuki, Antimutagenic structure modification of quinoline assessed by an in vivo mutagenesis assay using *lacZ*-transgenic mice, Mutat. Res. 414 (1998) 165–169.
[14] T. Suzuki, X. Wang, Y. Miyata, K.I. Saeki, A. Kohara, Y. Kawazoe, M. Hayashi, T. Sofuni, Hepatocarcinogen quinoline induces G:C to C:G transversions in the *cII* gene in the liver of lambda/*lacZ* transgenic mice (MutaMouse), Mutat. Res. 456 (2000) 73–81.
[15] R.S. Baker, A.M. Bonin, I. Stupans, G.M. Holder, Comparison of rat and guinea pig as sources of the S9 fraction in the *Salmonella*/mammalian microsome mutagenicity test, Mutat. Res. 71 (1980) 43–52.
[16] G.M. Seixas, B.M. Andon, P.G. Hollingshead, W.G. Thilly, The aza-arenes as mutagens for *Salmonella typhimurium*, Mutat. Res. 102 (1982) 201–212.
[17] S. Kumar, H.C. Sikka, S.K. Dubey, A. Czech, N. Geddie, C.X. Wang, E.J. LaVoie, Mutagenicity and tumorigenicity of dihydrodiols, diol epoxides, and other derivatives of benzo(*f*)quinoline and benzo(*h*)quinoline, Cancer Res. 49 (1989) 20–24.
[18] K.I. Saeki, H. Kawai, Y. Kawazoe, A. Hakura, Dual stimulatory and inhibitory effects of fluorine-substitution on mutagenicity: an extension of the enamine epoxide theory for activation of the quinoline nucleus, Biol. Pharm. Bull. 20 (1997) 646–650.
[19] M. Dong, I. Schmeltz, E. LaVoie, D. Hoffmann, Aza-arenes in the respiratory environment: analysis and assays for mutagenicity, in: P.W. Jones, R.I. Freudenthal (Eds.), Carcinogenesis: A Comprehensive Survey, vol. 3, Raven, New York, 1978, pp. 97–108.
[20] E.A. Adams, E.J. LaVoie, D. Hoffmann, Mutagenicity and metabolism of azaphenanthrenes, in: M.C. Cooke, A.J. Dennis (Eds.), Polynuclear Aromatic Hydrocarbons, Formation, Metabolism, and Measurement, Battelle Press, Columbus, OH, 1983, pp. 73–87.
[21] W.C. Summers, P.M. Glazer, D. Malkevich, Lambda phage shuttle vectors for analysis of mutations in mammalian cells in culture and in transgenic mice, Mutat. Res. 220 (1989) 263–268.
[22] E.J. Gunther, N.E. Murray, P.M. Glazer, High efficiency, restriction-deficient in vitro packaging extracts for bacteriophage lambda DNA using a new *E. coli* lysogen, Nucleic Acids Res. 21 (1993) 3903–3904.

[23] J.A. Gossen, A.C. Molijn, G.R. Douglas, J. Vijg, Application of galactose-sensitive *E. coli* strains as selective hosts for *LacZ*-plasmids, Nucleic Acids Res. 20 (1992) 3254.

[24] J.L. Jakubczak, G. Merlino, J.E. French, W.J. Muller, B. Paul, S. Adhya, S. Garges, Analysis of genetic instability during mammary tumor progression using a novel selection-based assay for in vivo mutations in a bacteriophage lambda transgene target, Proc. Natl. Acad. Sci. U.S.A. 93 (1996) 9073–9078.

[25] B. Sun, J.A. Heddle, The relationship between mutant frequency and time in vivo: simple predictions for any tissue, cell type, or mutagen, Mutat. Res. 425 (1999) 179–183.